Study of permeate flux behavior during photo-filtration using photocatalytic composite membranes

Duc-Trung Tran, Julie Mendret, Jean-Pierre Mericq, Catherine Faur, Stephan Brosillon

STUDY OF PERMEATE FLUX BEHAVIOR DURING PHOTO-FILTRATION USING PHOTOCATALYTIC COMPOSITE MEMBRANES

Duc-Trung Tran, Julie Mendret*, Jean-Pierre Méricq, Catherine Faur, Stephan Brosillon

Institut Européen des Membranes, IEM – UMR 5635, ENSCM, CNRS, CC047 Université de Montpellier, Montpellier, France

*Corresponding author: Julie Mendret; Institut Européen des Membranes, CC047 Université de Montpellier, 2 Place Eugène Bataillon, 34095 Montpellier Cedex 5, France ; *E-mail address*: julie.mendret@umontpellier.fr

Abstract

Photocatalytic PVDF-TiO_2 composite membranes were prepared by phase separation method. It was found that the membrane surface became more hydrophilic under UV irradiation, as characterized by a decrease in water contact angle after the membranes were exposed to UV. The photo-induced superhydrophilicity phenomenon of TiO_2 was attributed to such increase in membrane hydrophilicity. As a result, when filtration of pure water was performed under UV irradiation (photo-filtration), a gradual increase of permeate flux could be obtained over time. The role of UV irradiation mode on flux behavior during photo-filtration was investigated. Effective flux recovery could only be achieved under UV irradiances equal or higher than a threshold value. A flux "memory" effect was observed, in which the flux remained higher than its initial value for a certain duration even after irradiation was stopped, suggesting that the photo-filtration process could be more efficient if UV irradiation was operated in a on/off basis instead of a full-time one. In the scope of this study, five irradiation modes were selected, and based on the experimental data obtained from our lab-scale photo-filtration system, results of the cost/efficiency balance for a large-scale photo-filtration system were extrapolated. It was found that photo-filtration can be performed efficiently yet still economically.

Keywords: composite membranes; photo-filtration; hydrophilicity; UV irradiation; energy cost.

1. INTRODUCTION

Over the past decades, microfiltration (MF) and ultrafiltration (UF) have become more and more popular as advanced processes in water treatment. As such, the membranes used in these processes are desired to possess good properties like high flux, low fouling propensity, high rejection rate, as well as the ability to endure mechanical and chemical stress. Thanks to the good membrane-forming property as well as their mechanical, thermal and chemical stability, polymeric materials like polysulfone (PSf), polyethersulfone (PES) and polyvinylidenefluoride (PVDF) have always been the most popular choices among MF and UF membrane manufacturers [1]. However, most of these polymers are hydrophobic in nature, making them prone to fouling, which often causes significant declines in membrane performance especially in terms of the permeate flux, and consequently an increase in energy consumption [2]. As a consequence, the neat polymeric membranes have often been modified to develop new classes of membrane with stronger resistance to fouling and higher permeate flux. With the aid of nanotechnology, the incorporation of inorganic nanomaterials as fillers in the polymer matrix of the membranes has led to the expansion of composite membranes. For instance, nanosized inorganic fillers such as silver, silica, alumina, zeolite, carbon nanotubes or titanium dioxide have been mixed in the membrane structures by different methods to obtain various types of composite membranes with improved properties and performance [2–4].

Among those nanomaterials, titanium dioxide (TiO_2) can be considered the stand-out, as it has attracted great interest from researchers since its introduction in the 1960s, thanks to its excellent properties as a semiconductor [5]. Similar to many nanoparticles used in composite membranes, TiO_2 confers hydrophilicity to the membranes, which helps prevent fouling and promotes water transition. But what makes TiO_2 even more interesting, from a membrane performance point of view, is its photocatalytic behavior and photo-induced superhydrophilicity, both requiring the involvement of a UV source. While the well-known TiO_2 photocatalysis is associated with the breakdown of organic compounds or killing of bacteria, the more recently discovered phenomenon, photo-induced superhydrophilicity, is associated with the extremely high wettability (where the contact angle is less than 10^o) of a TiO_2 surface under UV irradiation [6]. To date, several hypotheses have been proposed to explain the mechanism of photo-induced superhydrophilicity. The first and widely accepted mechanism was proposed by Wang et al. [7], which relies on the generation of surface oxygen vacancies. Other mechanisms include the reconstruction of the Ti-OH bonds [8], the photo-oxidation of adsorbed hydrocarbons [9], or the combination of more than one mechanism [10]. While a

clear consensus on mechanism has not been elucidated, a consistent phenomenon was always observed: a strong decrease in contact angle when the TiO_2 surface was illuminated by UV light. For example, the water contact angle of TiO_2-coated glasses prepared by sol-gel method dropped to 0^o from an initial value of 35^o [11] and 72^o [7] after sufficient irradiation times. Since hydrophilicity is a much desired property for many membrane applications, especially in membranes for water purification, it would be very interesting if the photo-induced hydrophilicity property of TiO_2 can be transferred to composite membranes.

Thanks to the above properties, composite polymer-TiO_2 membranes have attracted a lot of interest among researchers [12]. Some demonstrated that by adding TiO_2 nanoparticles to the membranes, fouling mitigation could be achieved even without photocatalytic activities (i.e. without UV irradiation), thanks to significant changes in membrane structure and properties [13–18]. Others prepared composite polymer-TiO_2 membranes and studied their self-cleaning, anti-fouling, anti-bacterial performance under UV irradiation as well as their ability to degrade organic compounds via photocatalysis and found significant improvements compared to the neat polymeric membranes [19–26]. It is quite clear that in the cases where anti-fouling property was concerned, both the photocatalysis and photo-induced hydrophilicity effects occurred simultaneously and contributed to the enhancement. While photocatalysis generates strong oxidizing agents that can decompose contaminants, photo-induced hydrophilicity repels hydrophobic foulants from adsorbing on the membrane surface. Since the membrane becomes more resistant to fouling, its permeate flux, in turn, suffers less from decline. Yet interestingly, in the case where photo-induced hydrophilicity is in effect, the permeate flux could be improved not only because of reduced fouling, but also as a consequence of the membrane functionality itself. In other words, under the effect of photo-induced hydrophilicity, polymer-TiO_2 membranes have the ability to further enhance the transport of water molecules through its porous structure. This phenomenon, which often received few attention in studies of polymer-TiO_2 membranes, was briefly reported in our previous study [27]. Indeed, a spectacular rise in permeate flux (more than two times compared to the initial flux) was observed during pure water filtration of PVDF-TiO_2 membranes under continuous UV irradiation. Since membranes in water treatment are usually required to have high permeate flux and refrain from flux decline, this result is of particular interest because it opens the possibility to further improve the performance of TiO_2-doped polymeric membranes based on the interplay between membranes and UV irradiation. Indeed, to optimize the performance of photocatalytic membranes, besides improving the membrane properties by means such as alternating their morphology or photocatalyst content, varying the UV irradiation conditions

should also be considered as an effective method. A better control of UV irradiation method would reduce energy consumption and extend membrane lifetime, as intensive UV exposure may lead to degradation of the polymers. Thus, thorough investigation on this flux rising phenomenon are needed to further understand the potentials of photo-active membranes.

The overall goal of this study is to give more insights into the pure water flux behavior of photocatalytic composite membranes during filtration under continuous UV irradiation, which is also known as photo-filtration. Although studies dealing with the photo-wetting effect of TiO_2 were performed before, for example on TiO_2-coated commercial membrane [21], or on TiO_2-coated quartz fiber filters [28], detailed investigations of this effect on the membrane performance are more or less lacking. As such, the novelty and significance of this study lie within its three main tasks: (i) the mechanism behind the rise in pure water flux of blend composite membranes during photo-filtration was validated with concrete evidences of the increase in membrane hydrophilicity given by contact angle measurements under UV; (ii) the relationship between UV irradiation modes and permeate flux behavior was investigated in details for the first time; and (iii) the estimation of the energy consumed and operation costs associated with photo-filtration helped answer the question of whether this process can be both efficient and economical.

In this study, PVDF-TiO_2 composite membranes were prepared by the classic nonsolvent-induced phase separation (NIPS) method. PVDF was chosen as the polymer because of its excellent mechanical, thermal and chemical properties, and most importantly, its strong resistance to UV among other polymeric materials commonly used in membrane fabrication [27,29]. Since the aim of this study is not to investigate anti-fouling or degradation/separation performances of photocatalytic membranes, the feed source was restricted only to pure water to avoid potential inhibitory effects from other compounds on the photo-induced hydrophilicity effect. As for membrane characterization techniques, only water contact angle was performed as it is directly related to membrane hydrophilicity. Several photo-filtration conditions were tested and the permeate flux data were recorded. Using these experimental data, the energy consumption and water output for each photo-filtration conditions were calculated to have an outlook into the cost/efficiency balance of utilizing PVDF-TiO_2 membranes in photo-filtration, for a laboratory-scale closed system as well as an extrapolated large-scale system.

2. MATERIALS AND METHOD

2.1. Membrane preparation

All membranes in this study were prepared by the wet-NIPS method. PVDF (average molecular weight 275 kDa) was used as the polymer material. The solvent was N-N-Dimethylacetamide (DMAc, purity> 99.5%) and the polymeric additive was Polyethylene glycol (PEG, 200 Da). The nanoparticles were Aeroxide® TiO_2 P25 nanopowder (approx. 85% anatase and 15% rutile, size of c.a. 21 nm, purity > 99.5%). All chemicals were purchased from Sigma Aldrich and used as received.

The polymer dope solutions were prepared by mixing PVDF (20 wt%), TiO_2 (20 wt% TiO_2/PVDF, i.e. the TiO_2 concentration here is expressed as the mass ratio of TiO_2 to PVDF, or in other words, the fraction of TiO_2 in the membrane), PEG200 (5 wt%) in DMAc. For neat PVDF membranes, no TiO_2 amount was added. The mixtures were sonicated for 20 min and then agitated for 24 h at 50 °C with a magnetic stirrer to obtain a homogeneous solution. A Teflon® sheet was taped on top of a glass plate to form the casting support, where the solution (at 50°C) was cast upon, using an automated casting knife (Erichsen, Germany) set at 250 µm thickness and 50 $mm.s^{-1}$ velocity. The surface temperature of the casting plate was maintained at 50°C by means of a heating plate. After casting, the plate was immediately immersed in a 50°C deionized water bath (the exposure time of the cast film to ambient air before immersion was less than 10 s). The plate was left in the coagulation bath for 12 h, then the formed membrane was detached from the Teflon support, rinsed thoroughly with deionized water and stored in milliQ® water (18 MΩ.cm resistivity) at room temperature (20 ± 1°C) under dark condition.

2.2. Measurements of membrane contact angle

Water contact angle (WCA) of membranes were measured by the sessile drop method. Via a microsyringe, a drop of water (approx. 4 µL) was placed on the membrane surface. The image of the drop was captured by a video camera and then treated for WCA by the software imageJ (v1.46r). To study the effect of UV on membrane hydrophilicity, a UV lamp was equipped above the membrane so that its surface could receive irradiances of 0.5, 1 and 1.5 $mW.cm^{-2}$. At each irradiance, WCA was measured before irradiation and then immediately after 30 min of irradiation. In all cases, membrane samples were dried prior to tests and each result was averaged from at least six measurements performed on different locations of the membranes. WCA measurements were performed on both neat PVDF and PVDF-TiO_2 membranes.

2.3. Filtration with static UV irradiation

To verify the effect of photo-induced hydrophilicity on permeate flux, a dead-end membrane filtration system (Amicon, USA) with a cell volume of 50 mL and membrane surface area of

13.4 cm^2 was used. Pure water was filtrated at room temperature using a PVDF-TiO_2 membrane until a constant permeate flux was obtained. Following that, this membrane was removed from the cell and irradiated by UV for 30 min at an irradiance of 1 $mW.cm^{-2}$, then installed back to the dead-end cell to continue the pure water filtration. The permeate flux before and after irradiation was monitored and compared.

2.4. Photo-filtration

Photo-filtration tests were performed in a specifically designed crossflow filtration cell built with a Quartz window on top, so that the membrane could be illuminated continuously during the filtration by a UV lamp (Philips PL-S 9W, 365 nm). The membrane active filtration area was 30 cm^2 while the irradiated area was considered to be equal to the filtration area. A new membrane was always used for each test. Transmembrane pressure was provided by compressed air and controlled in the range of 0-1.5 bar. The feed solution was placed in a 5 L compressed tank and water was circulated at a cross-flow velocity ca. 0.1 $m.s^{-1}$ using a peristatic pump. Permeate flux was determined by monitoring the permeate mass via an electronic balance (Ohaus, USA, precision of 0.01 g) and recorded automatically by a computer software (Fig. 1). Prior to each test, the membrane was conditioned with pure water by increasing the pressure stepwise from 0.25 to 0.5, 0.75 and 1 bar every 15 min and finally to 1.25 bar for 30 min. All experiments were performed at room temperature (20 $\pm$ 1°C), while the permeate temperature was monitored and all permeate fluxes were subsequently presented at their corresponding values at 20°C.

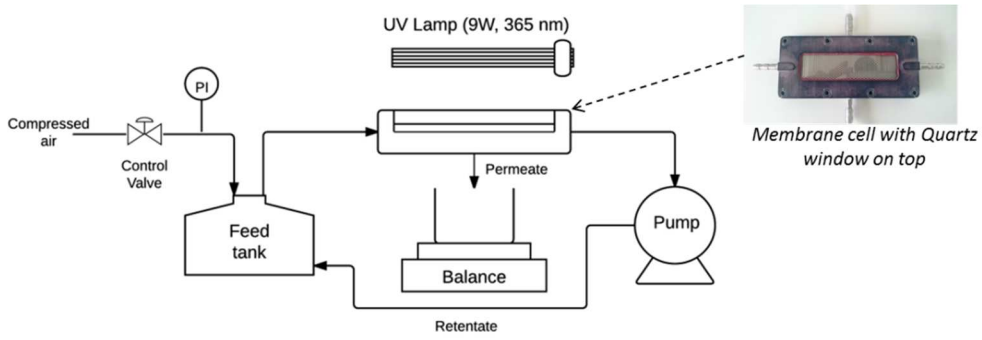

Fig. 1. Cross-flow filtration system equipped with UV irradiation.

With the goal being to study the behavior of pure water flux when photo-induced hydrophilicity effect is activated, milliQ® water and a constant transmembrane pressure of 1 bar were used in all experiments. To study the effect of light intensity, membranes were operated in dark condition for 60 min, followed by 120 min of photo-filtration under a range of irradiances from 0 to 1 $mW.cm^{-2}$. The UV irradiance at the membrane active surface was

controlled by adjusting the distance of the lamp to the filtration cell, and verified by a radiometer (UVA-365, Lutron, Taiwan). To study the effect of irradiation time, a fixed irradiance of 1 mW.cm^{-2} was maintained during the whole test, where the UV lamp was turned on and off periodically after some specific time periods (described in details in the relevant result sections), so that multiple irradiation cycles could be repeated.

3. RESULTS AND DISCUSSION

3.1. Discussion of photo-induced hydrophilicity on membrane permeate flux

As reported earlier, when PVDF-TiO_2 membranes were irradiated by UV during pure water filtration, the permeate flux increased gradually [27]. This phenomenon was not observed for neat PVDF membranes, and thus was theoretically assumed to occur due to the effect of the photo-induced superhydrophilicity of TiO_2 [21,30]. Since evidences of hydrophilicity change in PVDF-TiO_2 membranes under UV irradiation were still lacking, the effect of UV on membrane water contact angle is presented in Fig. 2.

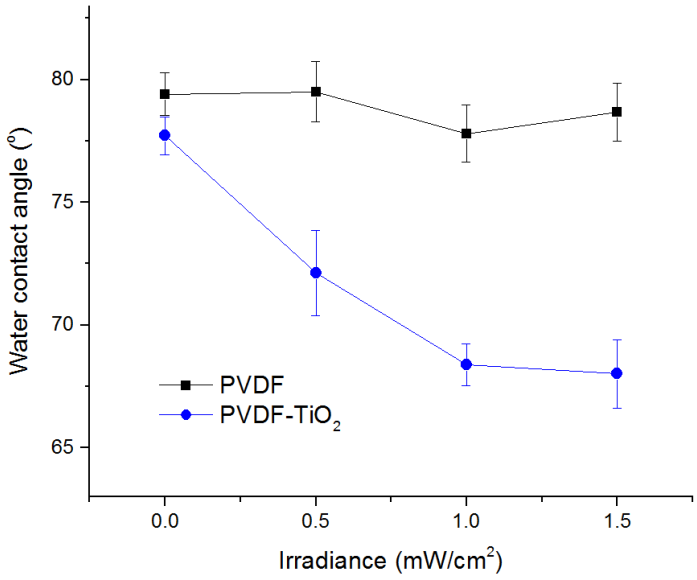

Fig. 2. Effect of UV irradiance on WCA of neat PVDF and PVDF-TiO_2 membranes.

As can be seen, for membranes without TiO_2, the differences in WCA before and after UV irradiation, regardless of the irradiance, were insignificant. On the other hand, for PVDF-TiO_2 membranes, from an initial WCA of 77.7±0.8°, after irradiation at 0.5, 1 and 1.5 mW.cm^{-2}, it dropped to 72.1±1.7, 68.4±0.9 and 68.0±1.4°, respectively. The WCA when membranes were irradiated at irradiances of 1 and 1.5 mW.cm^{-2} was almost the same, suggesting the surface hydrophilicity could not be increased further by UV light intensity. Nevertheless, there were significant decreases in WCA after the membranes were irradiated at all three irradiances

compared to the initial WCA. Although the effect of UV on hydrophilicity was not as strong as those reported for TiO_2 thin films, where the WCA could drop to virtually zero under sufficient irradiation conditions [7,31], it should be noted that such significant drop was achieved on pure TiO_2 surfaces. In our case, the membrane surface was a composite porous one comprising of TiO_2 nanoparticles mixed in PVDF matrix with a theoretical weight ratio of 1:5, so a strong decrease of WCA to superhydrophilic region (WCA < 10°) could not be expected. Nevertheless, the distribution of TiO_2 nanoparticles on the membrane surface as well as inside its porous structure was very uniform, as demonstrated for this membrane previously by energy-dispersive X-ray (EDX) mapping technique [27], suggesting that photo-induced hydrophilicity caused by TiO_2 would occur evenly across the membrane surface. As a result, it can be said that under UV irradiation, the surface of PVDF-TiO_2 membranes became more hydrophilic thanks to the photo-induced hydrophilicity effect of TiO_2.

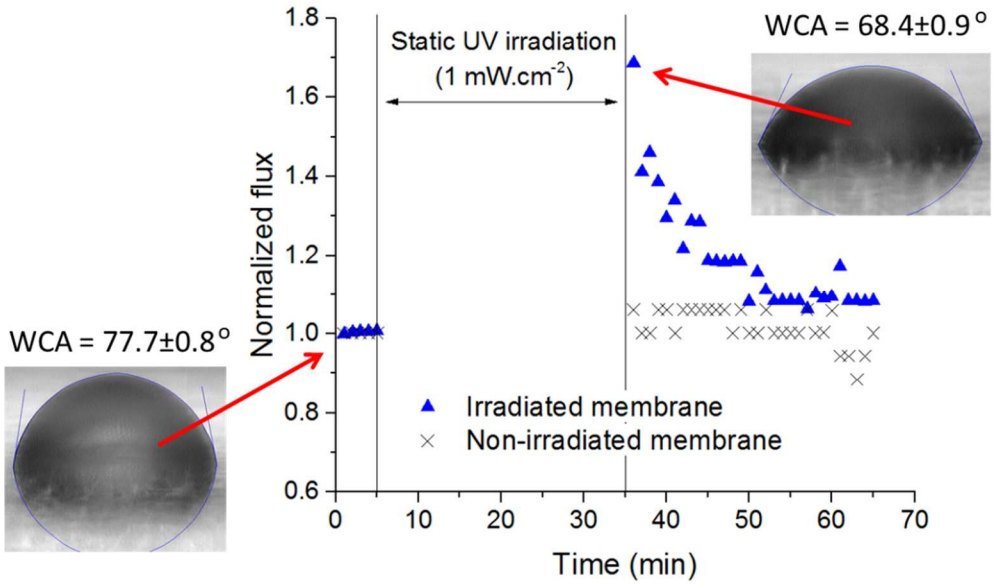

Fig. 3. Pure water flux before and after static UV irradiation. The two embedded images represent the WCA of the irradiated membrane before (left) and after (right) irradiation.

Then, the link between hydrophilicity and permeate flux was demonstrated in the flux test with static UV irradiation, as can be seen in Fig. 3. In this case, UV was not involved during the actual filtration test, but only in between the two flux tests, yet the immediate flux after static irradiation was 1.7 times higher than the one before. Afterwards, the flux quickly decreased, but was still 18% higher after 15 min, and 7% higher after 30 min, than the flux before irradiation. Such increase was not observed for the reference test in which the membrane was not irradiated during the 30-min interruption, suggesting that potential membrane decompression was not responsible for the flux increase observed in the irradiated membrane.

Generally, permeate flux depends on the porosity, pore interconnection, surface pore size, skin thickness and hydrophilicity of the membranes [2]. In this case, since other filtration conditions were unchanged, while the membrane surface hydrophilicity was proved to have increased, which was reflected by a 12% decrease in WCA, it can be hypothesized that such change in hydrophilicity was sufficient to induce a significant rise in pure water flux of PVDF-TiO_2 membranes. It should also be noted that during the course of the experiments performed in this study, the Fourier-transform infrared (FTIR) spectra of the membranes were analyzed. And it was found that the FTIR spectra of the pristine membrane and the irradiated membrane were identical, suggesting there was no degradation of the polymer at least during the duration of UV irradiation applied in this study. Similarly, potential leaching of TiO_2 nanoparticles during filtration was not detected, as analysis of trace metals in the permeate (by inductively coupled plasma mass spectrometry, ICP-MS) found virtually no amount of Ti. Thus, the possibility of flux increase due to potential changes in membrane structure or composition during UV irradiation is not likely.

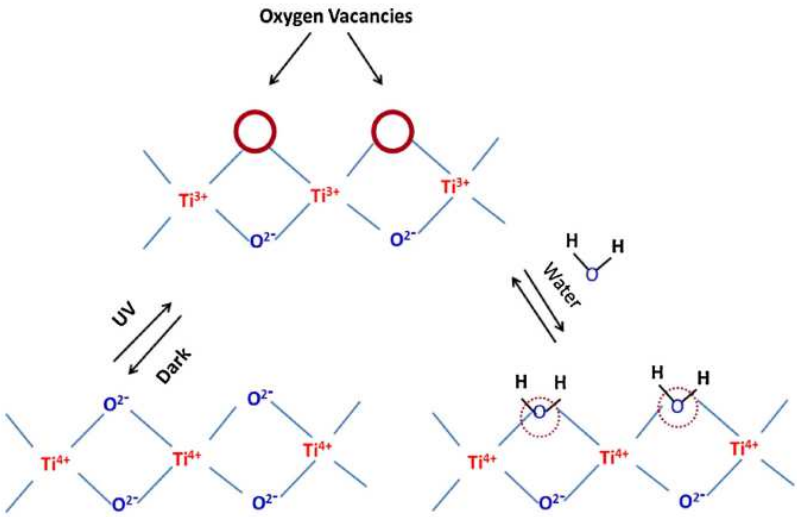

Fig. 4. Schematic mechanism of photo-induced hydrophilicity [10]

Although the mechanism of photo-induced hydrophilicity on membrane was discussed before [21], which was essentially based on the theory of oxygen vacancies proposed by Wang et al. [6], it usually referred to the selective adsorption of water molecules in contention with foulants on membrane surface for anti-fouling effect. As for the increase in permeate flux, it can be assumed as follows: upon UV irradiation, hydrophilic domains are formed on the membrane thanks to the chemisorbed water molecules at the oxygen vacancies. When exposed in aqueous environment, more and more layers of water are attracted via the hydrogen bonds and Van der Waals forces. These processes can be further intensified when

UV irradiance or irradiation time increases, as the number of hydrophilic domains increases, thus the membrane resistance to water transport keeps decreasing. Consequently, when transmembrane pressure is applied, these water layers can be moved much faster through the membrane structure, resulting in a gradual increase of permeate flux. This process may be further compounded by the fact that UV-A radiations have a certain penetration depth in solid matter, while the PVDF-TiO_2 membrane in this study was a porous mix-matrixed one having a thickness of about 70 µm. So it can be speculated that UV radiations may interact with TiO_2 nanoparticles inside the porous structure as well, inducing inner hydrophilicity, thus facilitating water transport not only at the membrane skin layer but also throughout its thickness.

3.2. Effect of UV irradiance on membrane permeate flux

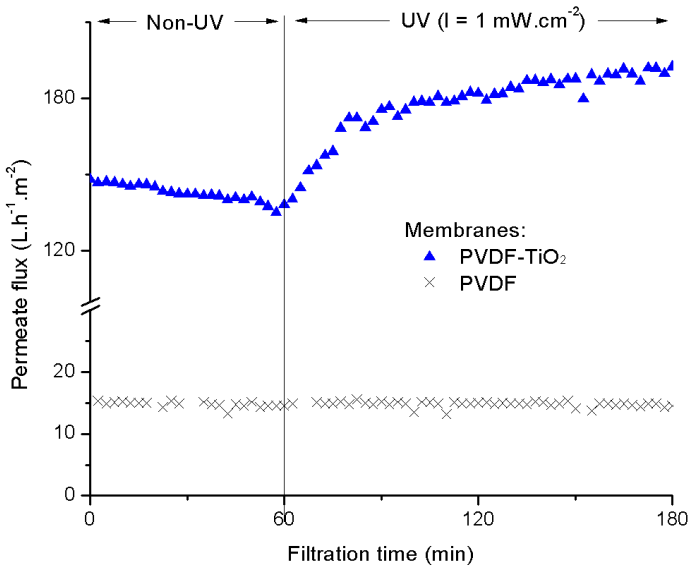

Fig. 5. Permeate flux of PVDF and PVDF-TiO2 membranes during photo-filtration.

A comparison of pure water flux between PVDF-TiO_2 and PVDF (without TiO_2) membranes during photo-filtration was first presented in Fig. 5. Both membranes were subject to 60 min of filtration without UV, followed by 120 min of filtration under a UV irradiance of 1 $mW.cm^{-2}$. Note that the initial flux of the PVDF-TiO_2 membrane was superior to that of the PVDF membrane: 148 to 15 $L.h^{-1}.m^{-2}$, despite that the difference in their WCA was very small (Fig. 2). In this case, the surface hydrophilicity played very little role and this ten-fold gap was mostly related to the difference between membrane structures, which is not covered within the scope of this study. It can be seen that for the neat PVDF membrane, the flux trend remained stable throughout the test whether UV was activated or not, whereas for the PVDF-TiO_2 membrane, the flux started to increase after irradiation. Thus, the possibility of UV directly inducing a flux increase, or UV interacting with the membrane polymer to cause pore

deformation, were both unlikely. Only with the presence of TiO_2 and consequently, the photo-induced hydrophilicity effect on the composite membrane, was a rise in flux observed.

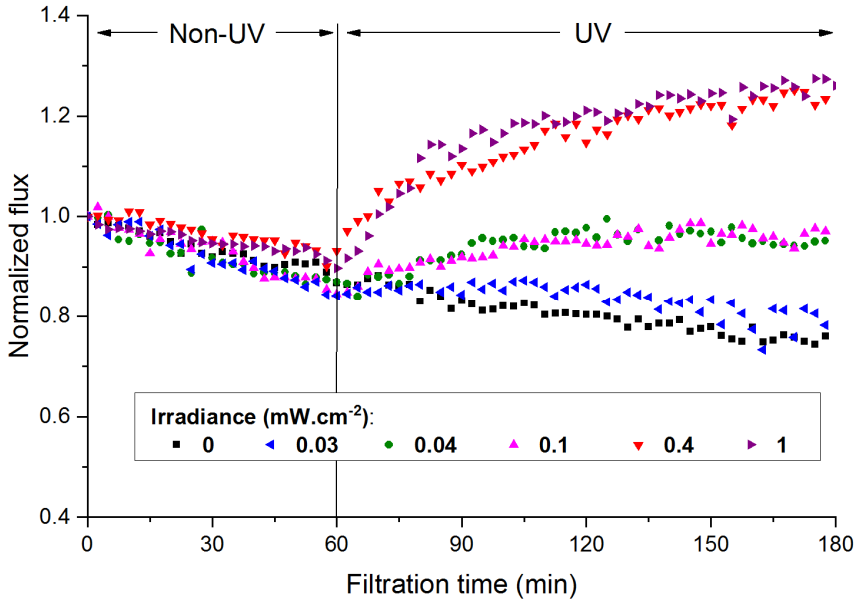

Fig. 6. Permeate flux of PVDF-TiO_2 membranes during photo-filtration at various irradiances.

As Fig. 2 indicates, increasing UV irradiance from 1 to 1.5 $mW.cm^{-2}$ did not cause further decrease in WCA, so it is unlikely that significant difference in permeate flux would be observed when photo-filtration was performed at these two irradiances. Thus, to explore the effective range of UV irradiance on PVDF-TiO_2 membranes for flux improvement, the irradiance range from 0 to 1 $mW.cm^{-2}$ was studied and results are presented in Fig. 6. For valid comparisons, membranes were subject to a period of 60 min filtration before UV was activated, so that at the end of the non-UV period, a flux decline of 10-15% was observed for all membranes. This decline could be attributed to the compaction which reduced the free volume inside the membranes, especially when these PVDF-TiO_2 membranes possessed high porosity (approx. 75%) and macrovoid structures in their cross-sectional morphology [27]. Obviously for the membrane not irradiated (I = 0 $mW.cm^{-2}$), the flux kept decreasing until the end of the experiment, reaching a value of about 75% of its initial flux. Yet upon the activation of UV, all other membranes showed signs of flux recovery at various degrees, depending on the magnitude of irradiance. After 120 min of photo-filtration, the pure water flux at irradiances of 0.4 and 1 $mW.cm^{-2}$ both saw strong increases of 25 and 30%, respectively, compared to their initial flux. At lower irradiances of 0.04 and 0.1 $mW.cm^{-2}$, although flux recoveries were considerable, the flux at the end could only reach to 95 and 98% of the initial flux, respectively.

Fig. 7 shows the percentage of increase when comparing the fluxes at the end of the non-UV period (60 min) and the end of the irradiation period (180 min). The relationship between UV irradiance and the degree of flux increase achieved via photo-induced hydrophilicity can be seen more clearly in this figure: beyond 0.04 mW.cm^{-2}, a positive correlation can be observed. Indeed, when irradiances increased, more photons were able to interact with TiO_2 nanoparticles on the surface or even in the pore walls of the membrane to provoke photo-reactions that induce hydrophilicity. Fig. 7 also explains why the flux behavior for the pair at 0.04 and 0.1 mW.cm^{-2}, and for the pair at 0.4 and 1 mW.cm^{-2}, looked similar in Fig. 6. The former was due to the small variation in UV irradiance, while the latter was down to a light saturation effect. This result is in agreement with what was suggested from the WCA measurements (Fig. 2), as the increase in UV irradiance above a certain level could not further induce more hydrophilicity on the membrane. As a result, the degree of flux increase was approaching a plateau at higher irradiances. In other words, there is a saturation point with regards to UV irradiance in photo-filtration.

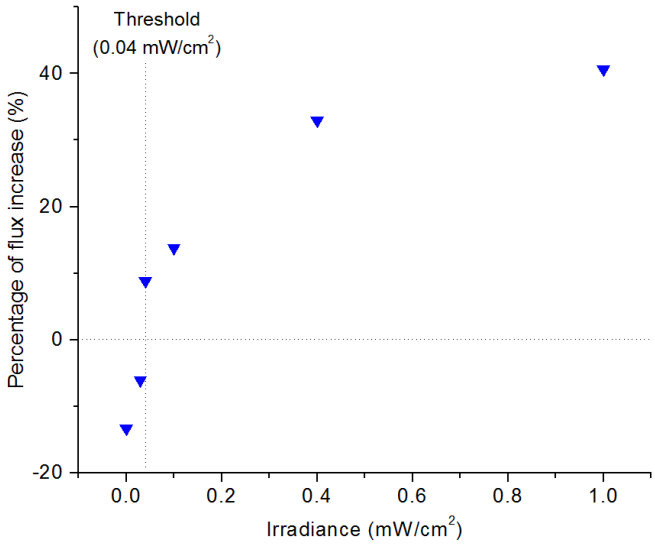

Fig. 7. Flux differences between the start and the end of the irradiation period.

In addition, a very important feature that can be observed from Fig. 6 and Fig. 7 is, when irradiance decreased to 0.03 mW.cm^{-2}, the flux recovery appeared to be not significant enough. Although the flux decline rate seemed to be slowed down during UV irradiation, a further 5% decrease on top of the 15% decrease after the 60 min non-UV period could be observed after 180 min. An apparent threshold seemed to exist for UV irradiance, at which a meaningful flux recovery can be expected for photo-filtration. In this case, the minimum irradiance required was 0.04 mW.cm^{-2} so that a flux decline of 10-15% could be fully recovered (Fig. 6). Below this value, the resulting flux increase from photo-induced hydrophilicity may be

too weak to offset the natural flux decline due to membrane compaction. It should also be noted that this value, which was determined in this particular experimental setup, is not a global constant, as the irradiance threshold may vary depending on the type of membranes or the source of irradiation. Indeed, as changes in TiO_2 concentration, TiO_2 distribution or the ability to resist compaction of the membranes may lead to very different pure water flux behaviors during photo-filtration. Thus, choosing a UV irradiance above the threshold (to ensure a significant flux improvement) and below the saturation point (to be more energy-efficient) is an important task in photo-filtration.

3.3. Effect of UV irradiation cycle on membrane permeate flux

While a positive effect to permeate flux was observed when the membranes were irradiated by UV, it might not be necessary to let them exposed to UV all the time. Instead, the membranes could be irradiated in cycles (UV/non-UV). The irradiance (I) of 1 $mW.cm^{-2}$, which was frequently applied by other TiO_2 researchers [11,32], was chosen to ensure hydrophilicity could be induced in a short period of time and accentuate the effect of irradiation cycle. Fig. 8 shows the flux behaviour of PVDF-TiO_2 membranes during photo-filtration in which the UV (fixed irradiance of 1 $mW.cm^{-2}$) was activated and deactivated successively every 30, 60 or 90 min.

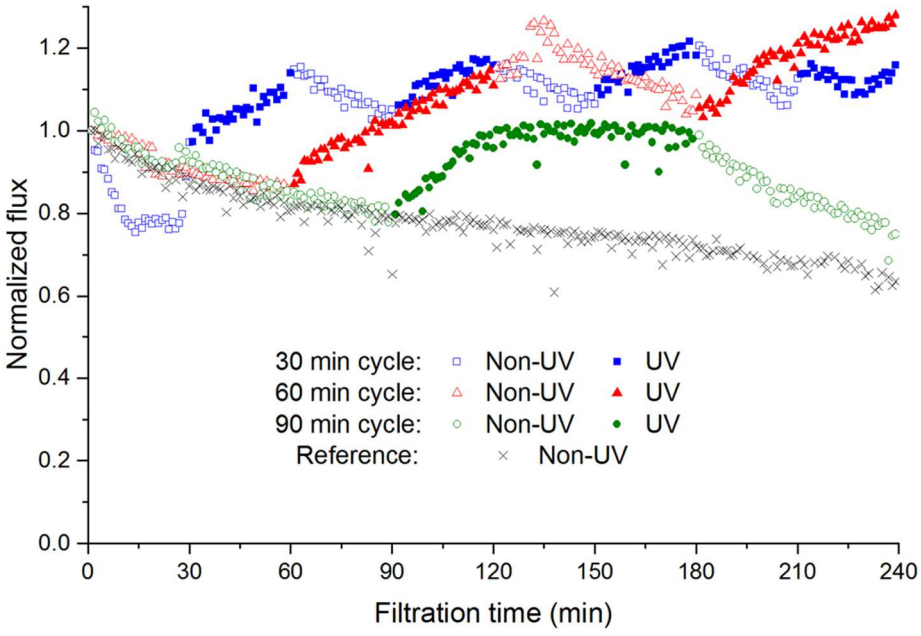

Fig. 8. Permeate flux behavior with different irradiation cycles (I = 1 $mW.cm^{-2}$).

It can be seen that regardless of the cycle time, when the membranes were irradiated intermittently in this manner, a step of flux rising always corresponded to the UV period while a step of flux falling corresponded to the non-UV period. The photo-induced hydrophilicity

effect remained active for each of the UV cycles during the total duration of the test (4 h), showing no signs of the membranes losing their photo-activities. Indeed, as stability study of PVDF-TiO_2 membranes prepared by blending method already showed that there was no leaching of TiO_2 from the membranes even after a month in operation under UV [33]. Looking at the 30 min cycle, despite the initial flux decrease, after just 30 minutes of irradiation the flux quickly recovered and even reached a value 15% higher than the initial flux. During the next non-UV cycle, a flux decrease occurred which could be considered as the gradual disappearance of the hydrophilic properties of TiO_2 materials in dark conditions [6,7,10]. However, the flux decrease rate of the second, third and fourth non-UV cycles was always lower than that of the first one (when UV had not been activated yet), and eventually, the flux at the end of each non-UV cycle was always higher than the initial flux J_0. In fact, after the first UV cycle, at no point during the remaining of the test had the flux dropped below the initial level. This suggests that it was not necessary to maintain UV irradiation all the time to maintain the flux of PVDF-TiO_2 membranes. The photo-induced hydrophilicity proved to have a lasting effect even after UV was deactivated. With respect to the longer UV cycles, the same trend also occurred with the 60 min cycle albeit with longer steps of flux rising and falling, while for the 90 min cycle the flux seemed to reach a plateau during the UV cycle where it could not be increased further despite continuous irradiation. All in all, excluding the 90 min cycle where there were two non-UV periods and only one UV period, a wide gap between the permeate flux of membranes irradiated and the reference membrane (not exposed to UV at all) can be seen in all cases after 4 h of filtration, demonstrating the strong influence of photo-induced hydrophilicity on the pure water flux of PVDF-TiO_2 membranes.

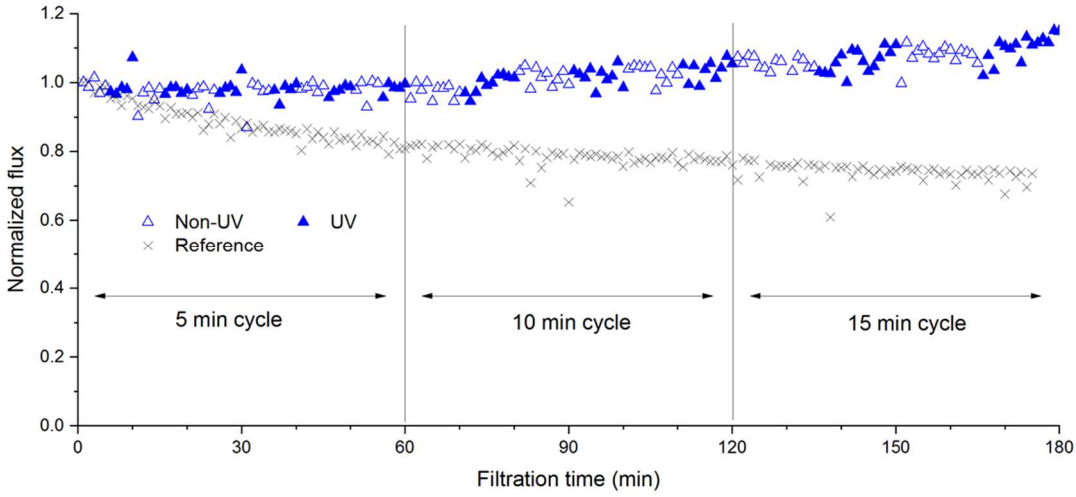

Fig. 9. Permeate flux behavior with UV cycles of short frequencies (I = 1 mW.cm^{-2}).

This so-called flux “memory” effect, which also explained the sudden rise in flux after static irradiation reported in Fig. 3, could be observed more clearly when decreasing the cycle time, as reported in Fig. 9. When UV was turned on and off every 5, 10 or 15 min, the shorter the cycle time, the smaller the flux decrease could be observed during the non-UV periods. In fact, photo-induced hydrophilicity remained significant for up to 10 min after the stop of irradiation, that flux decline observed during this period was almost non-existent. Again, in this case, the flux of the irradiated membrane always remained equal to or higher than its initial flux. However, due to the shorter irradiation cycles, the flux increase during UV periods was also less strong compared to the previous cases reported in Fig. 8. An explanation for the “memory” effect is the remaining of photo-induced hydrophilicity on the membranes after UV irradiation. Since this effect can last for a couple of days in the case of a TiO_2 film [10], it is supposedly possible that during filtration the increased hydrophilicity would last for a certain period after UV irradiation.

3.4. Optimization of permeate flux via UV irradiance and irradiation cycle

As the permeate flux behavior can be controlled by UV irradiance and irradiation cycle, the balance between membrane performance and energy consumption can be optimized by either of these factors, utilizing the flux “memory” effect. For example, the irradiation time can be shorter than the non-irradiation time, which not only reduces energy consumption but also decrease the rate of membrane aging. In Fig. 10, two types of unequal irradiation cycles were tested, where the irradiation time was only one third or half of the non-irradiation time. When the filtration cycles comprised of 30 min non-UV period and 10 min UV period, the general flux trend was a decreasing one, as the rise of flux in such a short time was not enough to offset the fall of flux during a period three times longer (Fig. 10a). Yet when the irradiation time was half of the non-irradiation time (15 and 30 min, respectively), an increasing trend was observed (Fig. 10b).

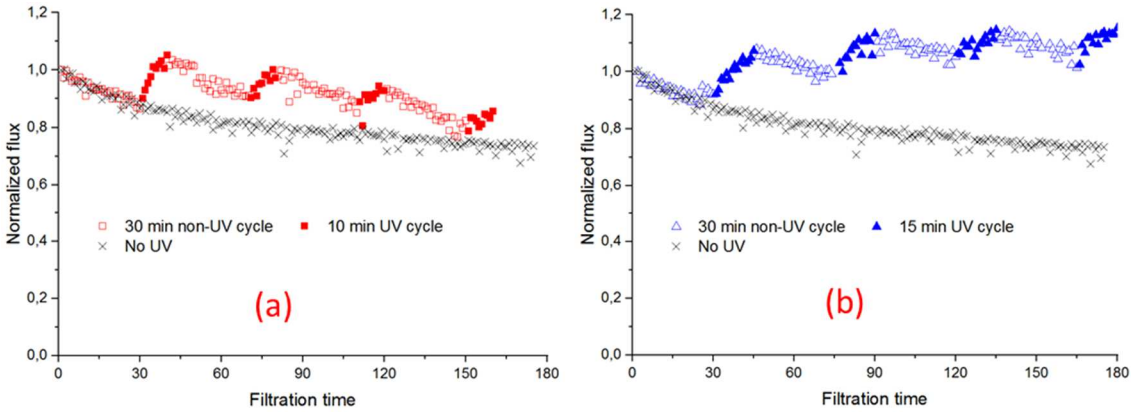

Fig. 10. Permeate flux behavior with unequal time of UV and non-UV cycles (I = 1 mW.cm^{-2}).

Similarly, the UV irradiance can be reduced from the standard one (1 mW.cm^{-2}) to a medium value (0.4 mW.cm^{-2}), and the threshold value (0.04 mW.cm^{-2}). The flux behaviour in each case is presented in Fig. 11. As can be seen, the flux behavior for the cases at 1 and 0.4 mW.cm^{-2} were almost the same, with the flux most of the time (after the first cycle) remaining above the initial level and reaching an increase of almost 20% at the end of the fourth cycle. These results are in agreement with the ones presented in Fig. 6, and also suggest that there exists an upper bound of irradiance, at which no significant flux improvements can be obtained even when irradiance is further increased. In addition, when the irradiance was decreased to the threshold level of 0.04 mW.cm^{-2}, the flux recovery effect was limited. This is similar to the corresponding case discussed in section 3.2, yet the difference is that when operating in irradiation cycle, the flux showed no signs of being able to recover to the initial value after the first non-UV cycle, and even suffered a slightly gradual decrease over time. Nevertheless, it was still an improvement compared to the flux of the reference membrane without any irradiation.

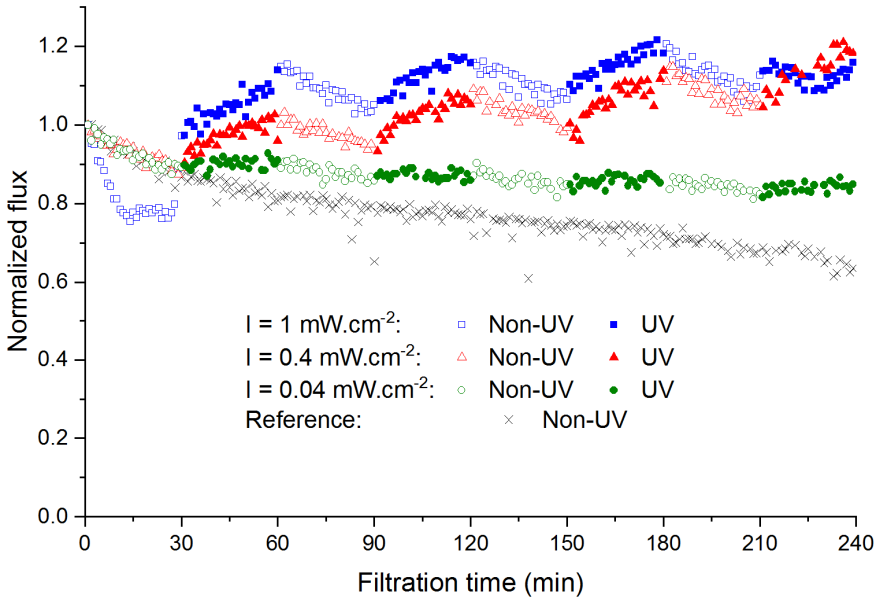

Fig. 11. Permeate flux behavior with 30 min cycle at different irradiances.

To make valid comparisons between the five irradiation modes presented, the distraction of flux decline by compaction can be eliminated by calculating the flux ratio between the irradiated membranes and the non-irradiated membrane (the reference). Thus, the average flux of each filtration cycle (UV or non-UV) was calculated and the evolution of said flux ratios is plotted in Fig. 12. It can be seen that except for mode 1 in which the irradiation time was insufficient, a constant increase of the irradiated membrane flux/non-irradiated membrane flux ratio could be obtained for all other modes. A flux ratio of about 1.7 was achieved at the end of cycle 8 for mode 3 and 4, showing the huge advantage of photo-filtration compared to normal filtration even when irradiation was only used for 50 percent of the time.

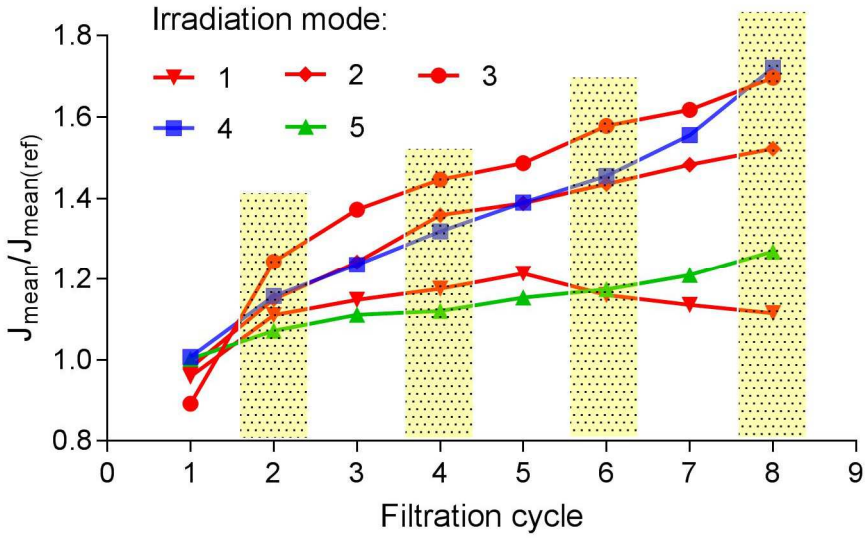

Fig. 12. Evolution of the average flux ratio between the irradiated membranes and the non-irradiated membrane. Cycles no. 2, 4, 6, 8 are irradiation cycles. Irradiances: 1 mW.cm^{-2} for mode 1, 2, 3; 0.4 mW.cm^{-2} for mode 4; 0.04 mW.cm^{-2} for mode 5. Irradiation cycles: 10 min UV + 30 min non-UV for mode 1; 15 min UV + 30 min non-UV for mode 2 ; 30 min UV + 30 min non-UV for mode 3, 4, 5.

3.5. Energy and cost/efficiency balance of photo-filtration

3.5.1. Energy consumption at laboratory scale

In the previous parts of this study, it was established that by employing photo-filtration, the water output of PVDF-TiO_2 membranes can be increased at the expense of some extra energy from UV irradiation, and the degree of increase depends on the irradiation modes. Therefore, the question of how much energy should be consumed to achieve the best efficiency remains. By calculating the extra water produced as a result of UV irradiation, which is the difference between the total permeate volume of a photo-filtration test and that of the normal filtration test (from this point referred to as the reference), a yield comparison between irradiation conditions can be obtained. Taking also into account the energy for UV irradiation, which can be deduced from the irradiance, and then the efficiency of the process can be evaluated. Table 1 presents the data for five different photo-filtration modes tested in this study. The shorter irradiation cycles (≤ 30 min) were used because as suggested in Section 3.3, it was more favourable to operate in short periods of non-UV to utilize most effectively the "memory" effect. It should be noted that to make these calculations, an initial permeate flux (J_0) of 150 L.h^{-1}.m^{-2} (which was the J_0 of the reference) was applied for all modes, instead of using the actual J_0 of each experiment (the actual J_0 were 180, 170, 175, 167, 160 L.h^{-1}.m^{-2} for mode 1, 2, 3, 4, 5, respectively) then the permeate volumes were calculated based on the normalized flux which has been recorded during the experiments. This assumption had to be made because the initial flux of each photo-filtration test was relatively different due to the nature of each membrane, thus taking the actual J_0 of each experiment would have produced random biases in the results, i.e. a membrane with higher J_o would generate more permeate than a membrane with lower J_o, then with the effect of UV, the difference in permeate volume between the two would even be more compounded, causing bias against the membrane with lower J_o.

Table 1. Energy consumption by irradiation and water output for different operating conditions of PVDF-TiO_2 membrane photo-filtration. Notes: [(1)] *permeate volume of the reference up to the corresponding filtration time (4 non-UV cycles + 4 UV cycles);* [(2)] *the*

difference between total permeate volume and reference volume, which corresponds to the extra water amount per hour produced as a result of photo-filtration; [3] *E/V = Irradiation energy/Total extra permeate volume, which denotes the amount of energy consumed by irradiation per unit volume of the extra permeate produced.*

Mode	Irradiance ($mW.cm^{-2}$)	UV cycle (min)	Non-UV cycle (min)	Total filtration time (min)	Total irradiation time (min)	**Irradiation energy ($W.h.m^{-2}$)**	Total permeate volume ($L.m^{-2}$)	Reference volume[1] ($L.m^{-2}$)	**Extra volume per hour [2] ($L.h^{-1}.m^{-2}$)**	**E/V[3] ($W.h.m^{-3}$)**
1	1	10	30	160	40	**6.7**	364	308	**21**	**119**
2	1	15	30	180	60	**10**	467	347	**40**	**83**
3	1	30	30	240	120	**20**	657	463	**48.5**	**103**
4	0.4	30	30	240	120	**8**	618	463	**38.75**	**52**
5	0.04	30	30	240	120	**0.8**	524	463	**15.25**	**13**

From Table 1, it is quite obvious that the extra water output by photo-filtration at the same irradiance increased linearly from 21 to 48.5 $L.h^{-1}.m^{-2}$ when the ratio of total irradiation time/total filtration time increased from 1:4 to 1:3 and 1:2 (mode 1, 2, 3). However a more economical way to achieve considerable improvement was to maintain a balanced irradiation condition (UV time = non-UV time) while reduce the irradiance (mode 3, 4, 5). For example, when comparing mode 3 and 4, the extra permeate volume only decreased by 20% (from 48.5 to 38.75 $L.h^{-1}.m^{-2}$) yet 60% of irradiation energy could be saved. To compare between irradiation conditions, the E/V ratio - which represents the amount of irradiation energy (W.h) needed to generate 1 m^3 of extra permeate from photo-filtration - can be looked at. From Table 1, it can be seen that when the threshold irradiance was applied (mode 5), the lowest E/V ratio was achieved and this value was significantly lower than those of other modes (4 times less than the second lowest E/V ratio and 10 times less than the highest). However, while certainly being the best in terms of energy-saving, it may not necessarily correspond to the overall best operating condition as the extra water output of mode 5 was also much lower than those of other modes. Thus, more considerations related to required output, total energy consumption and associated costs should be taken into account to identify suitable operating conditions for photo-filtration systems.

3.5.2. Cost estimation at large scale

As previously mentioned, the above comparisons are only valid for the laboratory-scale photo-filtration system used in our experiments. Although the goal was to relate the extra water

output produced by photo-filtration and the energy consumed by irradiation, it did not take into account the energy consumption of a traditional filtration system for pressurizing, as well as other practical elements of an open system such as con pressure loss, pump efficiency, etc. In addition, the investment costs for membrane and irradiation system have to be considered. Therefore, using the data in Table 1 and extrapolating to a large-scale open filtration system employing photocatalytic membranes, one can have a preliminary estimation of the operation as well as the investment costs of a photo-filtration system in comparison with a traditional filtration system. The estimation can be detailed as follows.

Considering a large-scale filtration system with a treatment capacity of 20,000 inhabitants and a discharge volume per person of 150 L per day, the feed flow (Qa) into the system is:

$$Qa\ (m^3.h^{-1}) = \frac{\text{"Capacity" x "Discharge"}}{24} \quad (1)$$

Assuming a conversion rate (Y) of 80%, then the permeate flow (Qp) is:

$$Qp\ (m^3.h^{-1}) = Y \times Qa \quad (2)$$

Note that Qa and Qp (125 and 100 $m^3.h^{-1}$, respectively) are indeed the same for all filtration modes. By dividing the total permeate volume by total filtration time (from Table 1), the mean permeate flux (J_{mean}) for the whole experimental duration in each mode can be obtained (presented in Table 2). The J_{mean}, in turn, gives the membrane surface area (A) required to provide such permeate flow:

$$A\ (m^2) = \frac{Qp}{J_{mean}} \quad (3)$$

Using a polymeric membrane cost of 100 $USD.m^{-2}$ and lifetime of 5 years [34], then the cost for photocatalytic membranes can be calculated from the membrane area. To be more rigorous in terms of economics, the interest rate - assuming to be 7% per year [35] can also be taken into account, so that the daily capital cost for membranes is:

$$\text{Daily membrane cost } (USD.d^{-1}) = A \times 100 \times 7\% \times \frac{1}{[1-(1+7\%)^{-5}] \times 365} \quad (4)$$

Since photo-filtration system requires irradiation, the cost for UV lamps has to be taken into account as well. However, as the required number of lamps heavily depends on the design of the membrane shape and module, in this study, only a simplified estimation based on our experimental conditions was provided to give an overall idea of the investment cost for photo-filtration system.

Assuming the UV lamp has a useful working life of 15000 h, its lifetime in the photo-filtration system (t_L) would differ depending on the irradiation mode and can be calculated as follows:

$$t_L \text{ (years)} = \frac{18000}{t_{UV} \times 365} \quad (5)$$

in which t_{UV} is the irradiation time per day, which is calculated by multiplying the time proportion of a UV cycle to a full photo-filtration cycle (which are 1/4 for mode 1, 1/3 for mode 2 and 1/2 for mode 3, 4, 5) with 24 h.

Assuming each lighting unit can cover a membrane area of 0.6 m^2 (estimated from our experimental condition) and costs 6.4 USD (average cost for a UV-A light bulb), the daily capital cost for UV lamp, with a 7% interest rate taken into account, is:

$$\text{Daily UV lamp cost (USD.d}^{-1}) = \frac{A}{0.3} \times 10 \times 7\% \times \frac{1}{\left[1-(1+7\%)^{-t_L}\right] \times 365} \quad (6)$$

For energy consumption, considering that the system operates at the same pressure with the one in this study (ΔP = 1 bar), and assuming the pump efficiency (η_p) for both feed and recirculation flow is 75% and a pressure loss (dP) of 70% [36], the daily energy for feed pressure (Wp) and recirculation (Wr) can be calculated as:

$$Wp \text{ (kWh)} = \frac{Qa \times \Delta P \times 24}{\eta_p} \quad (7)$$

$$\text{and } Wr \text{ (kWh)} = \frac{Qr \times dP \times 24}{\eta_p} = \frac{R \times Qa \times dP \times 24}{\eta_p} \quad (8)$$

in which Qr is the recirculation flow (Qr = R x Qa) and R is the recirculation rate, which can be chosen at 800%.

The daily total energy for pumping (W) is then the sum of Wp and Wr:

$$W \text{ (kWh)} = Wp + Wr \quad (9)$$

It is obvious that for daily pumping energy, the consumption in all modes, including the reference, are always the same (which is calculated at 733.33 kWh). The differences in total energy consumption are only caused by the daily energy for UV irradiation (W_{UV}), which can be calculated based on the irradiances (I), membrane surface area (A), the irradiation time per day (t_{UV}) and the UV lamp efficiency (η_{UV} = 40% for the type of lamp used in this study):

$$W_{UV} \text{ (kWh)} = \frac{I \times A \times t_{UV}}{\eta_{uv}} \quad (10)$$

The key figures of the investment and operation costs associated with the extrapolated photo-filtration system are presented in Table 2. The detailed calculations can be provided in the Supporting Information sheet.

Table 2. Energy consumption and associated costs of a simulated large-scale photo-filtration system (capacity 20000 inhabitants/day).

		Reference	Mode 1	Mode 2	Mode 3	Mode 4	Mode 5
Mean permeate flux	$L.h^{-1}.m^{-2}$	115.7	136.5	155.7	164.3	154.5	131.0
Membrane surface	m^2	864.3	732.6	642.3	608.6	647.2	763.4
Daily membrane cost	$USD.d^{-1}$	**57.8**	**49.0**	**42.9**	**40.7**	**43.2**	**51.0**
% compared to reference	*%*		***-15.2***	***-25.7***	***-29.6***	***-25.1***	***-11.7***
Daily UV lamp cost	$USD.d^{-1}$	0.0	4.8	5.4	7.4	7.8	9.2
Daily investment cost	$USD.d^{-1}$	**57.8**	**53.8**	**48.3**	**48**	**51.1**	**60.2**
% compared to reference	*%*		***-6.9***	***-16.3***	***-16.8***	***-11.6***	***+4.3***
Daily pumping energy	*kWh*	733.3	733.3	733.3	733.3	733.3	733.3
Daily irradiation energy	*kWh*	0.0	109.9	128.5	182.6	77.7	9.2
Daily total energy	*kWh*	733.3	843.2	861.8	915.9	811.0	742.5
Daily operation cost*	$USD.d^{-1}$	**51.3**	**59.0**	**60.3**	**64.1**	**56.8**	**52.0**
% compared to reference	*%*		***+15.0***	***+17.5***	***+24.9***	***+10.6***	***+1.2***
Daily total cost	$USD.d^{-1}$	**109.1**	**112.8**	**108.7**	**114.1**	**107.8**	**112.2**
% compared to reference	*%*		***+3.4***	***-0.4***	***+2.8***	***-1.1***	***+2.9***

** The electricity price is chosen at 0.07 USD/kWh (average industrial rate in 2017 in the U.S.)*

Table 2 clearly shows that, to process the same volume of feed (3000 $m^3.d^{-1}$, in our hypothetical case), employing photo-filtration would help reduce the expense for membrane greatly (almost 30% for mode 3, and about 25% for mode 2 and 4), thanks to the superior water output with irradiation. The requirement for irradiation generates extra cost for UV lamps, which more or less neutralizes the advantage from the reduced membrane cost, except for mode 2 and 4. Slight reductions in total investment cost can still be obtained when these irradiation modes are used. On the other hand, due to the need for UV irradiation, energy consumption and associated operation costs have to increase for photo-filtration (up to 25% for mode 3 as the highest, and a slight increase of 1.5% for mode 5 as the lowest).

Combining the investment and operation costs together, the total cost for photo-filtration is obtained. Depending on the case there are either a slight increases of the total cost or slight reductions of the total cost. This result more or less reflects our approach in optimizing the

efficiency of photo-filtration by varying the irradiation mode (by either reducing the light intensity, or using irradiation cycles with irradiation time shorter than non-irradiation time).

This result is very important because, as a first approach, it seems to indicate that this new photo-filtration technology does not involve huge increase of the cost of the treatment. It should be mentioned that economic calculations are rarely in favour of emerging technology. In addition, the efficiency of the system can still be further optimized, either by further optimizing the irradiation mode, improving the membrane photo-performance, creative design of the membrane module, or using better irradiation technology (UVA LED); and (ii) in this study, the cost/efficiency balance of photo-filtration was only assessed based on the volumic water output of the system, yet the photo-induced hydrophilicity is only one of the two major properties of polymer-TiO_2 membranes. In fact, UV irradiation activates the self-cleaning and treatment capacity of the membrane, which is another significant advantage. Thus, the overall economic outlook of photo-filtration is still very promising.

CONCLUSIONS

In this study, the effects of photo-induced hydrophilicity on pure water flux behavior of PVDF-TiO_2 membranes were investigated thoroughly by means of photo-filtration. It was demonstrated that PVDF-TiO_2 membranes became more hydrophilic upon UV irradiation, evidenced by a decrease of 7-12% in WCA depending on the irradiance level. The increased hydrophilicity was responsible for the rise in pure water flux during photo-filtration, as layers of water were more easily attracted and quickly transported through the membranes. No evidence of polymer degradation under UV exposure was found during the course of this study. Interestingly, when photo-filtration was operated in cycle mode, even after the irradiation was stopped, the flux rising effect still remained for a while. This so-called flux "memory" effect was particularly discernible when the duration of the non-UV cycles was short. Thus it was suggested that photo-filtration should be performed in short cycles comprising of non-UV and UV periods successively in order to maintain a good permeate flux level while continuous membrane exposure to UV can be avoided. In addition, to optimize the efficiency of photo-filtration, the light intensity should fall between the threshold level (determined at 0.04 $mW.cm^{-2}$ in this study) where significant flux recovery can be obtained, and the saturation level where the flux improvement is insignificant compared to the increase in energy consumption.

Based on these findings, the irradiation mode in photo-filtration was varied, by either reducing the irradiation time or reducing the UV irradiance, to study the permeate flux behavior of the

membrane and optimize the efficiency of the process. Five irradiation modes were selected to analyze the cost/efficiency balance of photo-filtration when extrapolated to a large-scale open system. It was found that the higher water output produced by photo-filtration help decrease the required membrane areas greatly, thus reducing the investment cost for membrane. The total cost of photo-filtration is the same order than a traditional filtration system, the advantages of photo-filtration in water treatment, in terms of its high water output and also its treatment capacity, are still significant, especially when this filtration method can still be further optimized.

Nevertheless, as a first study of this kind, only the pure water output of PVDF-TiO_2 membrane was evaluated for its photo-filtration performance. In reality, the membranes are not operated in such ideal condition and inhibitory elements in the feed source may limit the effectiveness of photo-induced hydrophilicity. Thus more follow-up studies are required to comprehensively assess the efficiency of photo-filtration systems, as well as the long-term stability of photocatalytic membranes under UV irradiation.

References

[1] B. Van Der Bruggen, C. Vandecasteele, T. Van Gestel, W. Doyen, R. Leysen, A review of pressure-driven membrane processes in wastewater treatment and drinking water production, Environ. Prog. 22 (2003) 46–56.

[2] P.S. Goh, B.C. Ng, W.J. Lau, A.F. Ismail, Inorganic Nanomaterials in Polymeric Ultrafiltration Membranes for Water Treatment, Sep. Purif. Rev. 44 (2015) 216–249.

[3] J. Kim, B. Van der Bruggen, The use of nanoparticles in polymeric and ceramic membrane structures: Review of manufacturing procedures and performance improvement for water treatment, Environ. Pollut. 158 (2010) 2335–2349.

[4] J.H. Jhaveri, Z.V.P. Murthy, A comprehensive review on anti-fouling nanocomposite membranes for pressure driven membrane separation processes, Desalination. 379 (2016) 137–154.

[5] A. Fujishima, T.N. Rao, D.A. Tryk, Titanium dioxide photocatalysis, J. Photochem. Photobiol. C Photochem. Rev. 1 (2000) 1–21.

[6] R. Wang, K. Hashimoto, A. Fujishima, M. Chikuni, E. Kojima, A. Kitamura, M. Shimohigoshi, T. Watanabe, Photogeneration of highly amphiphilic TiO2 surfaces, Adv. Mater. 10 (1998) 135–138.

[7] R. Wang, K. Hashimoto, A. Fujishima, M. Chikuni, E. Kojima, A. Kitamura, M. Shimohigoshi, T. Watanabe, Light-induced amphiphilic surfaces, Nature. 388 (1997) 431–432.

[8] N. Sakai, A. Fujishima, T. Watanabe, K. Hashimoto, Quantitative evaluation of the photoinduced hydrophilic conversion properties of TiO2 thin film surfaces by the reciprocal of contact angle, J. Phys. Chem. B. 107 (2003) 1028–1035.

[9] T. Zubkov, D. Stahl, T.L. Thompson, D. Panayotov, O. Diwald, J.T. Yates, Ultraviolet light-induced hydrophilicity effect on TiO2(110)(1x1). Dominant role of the photooxidation of adsorbed hydrocarbons causing wetting by water droplets, J. Phys. Chem. B. 109 (2005) 15454–15462.

[10] S. Banerjee, D.D. Dionysiou, S.C. Pillai, Self-cleaning applications of TiO2 by photo-induced hydrophilicity and photocatalysis, Appl. Catal. B-Environmental. 176 (2015) 396–428.
[11] T. Watanabe, A. Nakajima, R. Wang, M. Minabe, S. Koizumi, A. Fujishima, K. Hashimoto, Photocatalytic activity and photoinduced hydrophilicity of titanium dioxide coated glass, Thin Solid Films. 351 (1999) 260–263.
[12] S.W. Leong, A. Razmjou, K. Wang, K. Hapgood, X.W. Zhang, H.T. Wang, TiO2 based photocatalytic membranes: A review, J. Memb. Sci. 472 (2014) 167–184.
[13] T.H. Bae, T.M. Tak, Effect of TiO2 nanoparticles on fouling mitigation of ultrafiltration membranes for activated sludge filtration, J. Memb. Sci. 249 (2005) 1–8.
[14] X.C. Cao, J. Ma, X.H. Shi, Z.J. Ren, Effect of TiO2 nanoparticle size on the performance of PVDF membrane, Appl. Surf. Sci. 253 (2006) 2003–2010.
[15] J.H. Li, Y.Y. Xu, L.P. Zhu, J.H. Wang, C.H. Du, Fabrication and characterization of a novel TiO2 nanoparticle self-assembly membrane with improved fouling resistance, J. Memb. Sci. 326 (2009) 659–666.
[16] S.J. Oh, N. Kim, Y.T. Lee, Preparation and characterization of PVDF/TiO2 organic-inorganic composite membranes for fouling resistance improvement, J. Memb. Sci. 345 (2009) 13–20.
[17] Y.H. Teow, A.L. Ahmad, J.K. Lim, B.S. Ooi, Preparation and characterization of PVDF/TiO2 mixed matrix membrane via in situ colloidal precipitation method, Desalination. 295 (2012) 61–69.
[18] Y.H. Teow, B.S. Ooi, A.L. Ahmad, Fouling behaviours of PVDF-TiO2 mixed -matrix membrane applied to humic acid treatment, J. Water Process Eng. 15 (2017) 89–98.
[19] O.T. Alaoui, Q.T. Nguyen, C. Mbareck, T. Rhlalou, Elaboration and study of poly(vinylidene fluoride)-anatase TiO2 composite membranes in photocatalytic degradation of dyes, Appl. Catal. a-General. 358 (2009) 13–20.
[20] R.A. Damodar, S.J. You, H.H. Chou, Study the self cleaning, antibacterial and photocatalytic properties of TiO2 entrapped PVDF membranes, J. Hazard. Mater. 172 (2009) 1321–1328.
[21] S.S. Madaeni, N. Ghaemi, A. Alizadeh, M. Joshaghani, Influence of photo-induced superhydrophilicity of titanium dioxide nanoparticles on the anti-fouling performance of ultrafiltration membranes, Appl. Surf. Sci. 257 (2011) 6175–6180.
[22] A. Rahimpour, M. Jahanshahi, B. Rajaeian, M. Rahimnejad, TiO2 entrapped nano-composite PVDF/SPES membranes: Preparation, characterization, antifouling and antibacterial properties, Desalination. 278 (2011) 343–353.
[23] H.P. Ngang, B.S. Ooi, A.L. Ahmad, S.O. Lai, Preparation of PVDF-TiO2 mixed-matrix membrane and its evaluation on dye adsorption and UV-cleaning properties, Chem. Eng. J. 197 (2012) 359–367.
[24] H.C. Song, J.H. Shao, Y.L. He, B. Liu, X.Q. Zhong, Natural organic matter removal and flux decline with PEG-TiO2-doped PVDF membranes by integration of ultrafiltration with photocatalysis, J. Memb. Sci. 405 (2012) 48–56.
[25] N.A.M. Nor, J. Jaafar, A.F. Ismail, M.A. Mohamed, M.A. Rahman, M.H.D. Othman, W.J. Lau, N. Yusof, Preparation and performance of PVDF-based nanocomposite membrane consisting of TiO2 nanofibers for organic pollutant decomposition in wastewater under UV irradiation, Desalination. 391 (2016) 89–97.
[26] A. Munoz-Bonilla, A. Kubacka, M. Fernandez-Garcia, M. Ferrer, M. Fernandez-Garcia, M.L. Cerrada, Visible and ultraviolet antibacterial behavior in PVDF-TiO2 nanocomposite films, Eur. Polym. J. 71 (2015) 412–422.
[27] J.P. Mericq, J. Mendret, S. Brosillon, C. Faur, High performance PVDF-TiO2 membranes for water treatment, Chem. Eng. Sci. 123 (2015) 283–291.
[28] M. Hatat-Fraile, R. Liang, M.J. Arlos, R.X. He, P. Peng, M.R. Servos, Y.N. Zhou,

Concurrent photocatalytic and filtration processes using doped TiO2 coated quartz fiber membranes in a photocatalytic membrane reactor, Chem. Eng. J. 330 (2017) 531–540.
[29] S.S. Chin, K. Chiang, A.G. Fane, The stability of polymeric membranes in a TiO2 photocatalysis process, J. Memb. Sci. 275 (2006) 202–211.
[30] J. Mendret, M. Hatat-Fraile, M. Rivallin, S. Brosillon, Hydrophilic composite membranes for simultaneous separation and photocatalytic degradation of organic pollutants, Sep. Purif. Technol. 111 (2013) 9–19.
[31] A. Langlet, S. Permpoon, D. Riassetto, G. Berthome, E. Pernot, J.C. Joud, Photocatalytic activity and photo-induced superhydrophilicity of sol-gel derived TiO2 films, J. Photochem. Photobiol. a-Chemistry. 181 (2006) 203–214.
[32] M. Takeuchi, K. Sakamoto, G. Martra, S. Coluccia, M. Anpo, Mechanism of photoinduced superhydrophilicity on the TiO2 photocatalyst surface, J. Phys. Chem. B. 109 (2005) 15422–15428.
[33] H. Dzinun, M.H.D. Othman, A.F. Ismail, M.H. Puteh, M.A. Rahman, J. Jaafar, Stability study of PVDF/TiO2 dual layer hollow fibre membranes under long-term UV irradiation exposure, J. Water Process Eng. 15 (2017) 78–82.
[34] G. Owen, M. Bandi, J.A. Howell, S.J. Churchhouse, Economic-Assessment of Membrane Processes for Water and Waste-Water Treatment, J. Memb. Sci. 102 (1995) 77–91.
[35] A. Suarez, P. Fernandez, J.R. Iglesias, E. Iglesias, F.A. Riera, Cost assessment of membrane processes: A practical example in the dairy wastewater reclamation by reverse osmosis, J. Memb. Sci. 493 (2015) 389–402.
[36] X.Y. Wang, S.H. Davies, S.J. Masten, Analysis of energy costs for catalytic ozone membrane filtration, Sep. Purif. Technol. 186 (2017) 182–187.

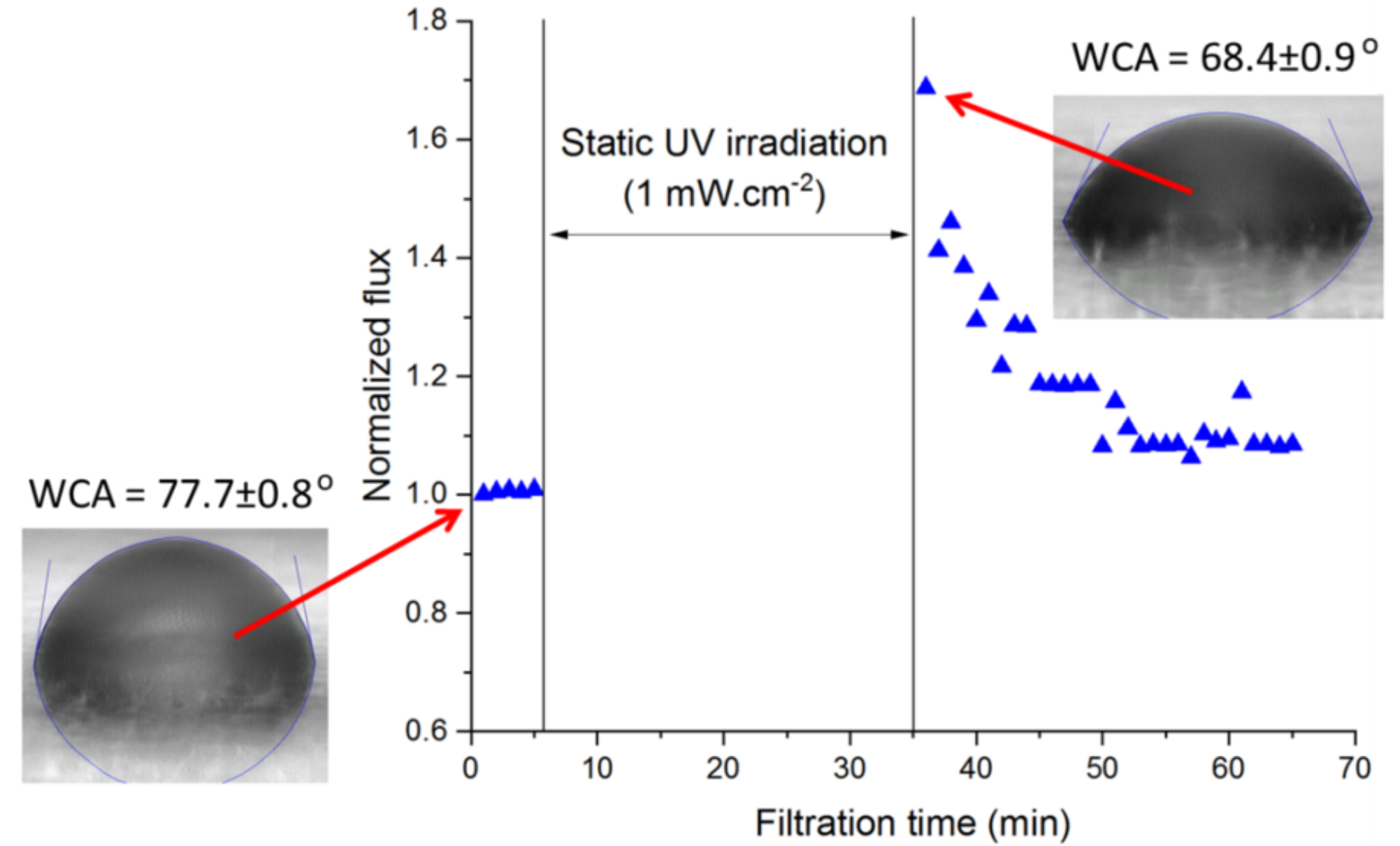
WCA = 68.4±0.9°
Static UV irradiation
(1 mW.cm-2)
WCA = 77.7±0.8°
Normalized flux
1.8
1.6
1.4
1.2
1.0
0.8
0.6
0
10
20
30
40
50
60
70
Filtration time (min)